CLUSTERS OF INTRAMEMBRANE PARTICLES ASSOCIATED WITH BINDING SITES FOR α-BUNGAROTOXIN IN CULTURED CHICK MYOTUBES

S. A. COHEN and D. W. PUMPLIN

From the Laboratory of Developmental Neurobiology and the Section of Functional Neuroanatomy, National Institutes of Health, Bethesda, Maryland 20205, and the Department of Anatomy, University of Maryland Medical School, Baltimore, Maryland 21201. Dr. Cohen's present address is the Department of Pathology, Albert Einstein College of Medicine, Bronx, New York 10461.

ABSTRACT

Developing chick myotubes in tissue culture were freeze-fractured to yield complementary replicas of large areas of membrane. Regions of muscle fibers with high concentrations of acetylcholine receptors were identified by binding of fluorescent-labeled α-bungarotoxin. Membranes in such regions contained clusters of large (100 Å Diam) angular particles, similar in appearance to particles found in postsynaptic membranes of cholinergic synapses. Particles appeared in apposing areas of cytoplasmic and external leaflets but were more prevalent in the cytoplasmic leaflet. The areas of high particle concentration were coextensive with the fluorescence due to bound toxin.

Treatment of cultures with tetrodotoxin increased the size of fluorescent spots and areas of high concentration of particles relative to those found in control cultures.

In muscle cultures grown in the presence of spinal cord explants, some neurites contacted and innervated nearby myotubes. Intense fluorescence due to binding of α-bungarotoxin was present at portions of such neurite-myotube contacts. At these same portions, a high concentration of large angular particles was present in the sarcolemma adjacent to the neurite. In addition, an ordered arrangement of large particles was seen in the cytoplasmic leaflet of the neuronal plasmalemma directly apposing the muscle. The possible significance of these arrangements is discussed.

Clusters on myotubes tended to be larger (contain more particles) when they occurred in groups, defined as three or more clusters with an intercluster distance of <0.5 μm. Clusters were also larger in myotubes treated with tetrodotoxin and in myotubes adjacent to some neurites in nerve-muscle cocultures.

Several depressions containing particles similar to those in the clusters were found in the sarcolemma. The implications of these depressions are discussed in light of current theories of incorporation of proteins into cell membranes.

J. CELL BIOLOGY © The Rockefeller University Press · 0021-9525/79/08/0494/23 $1.00
Volume 82 August 1979 494–516

KEY WORDS intramembrane particles · acetylcholine receptors · tissue culture · neuromuscular junctions · receptor aggregation

Acetylcholine receptors (AChRs) are highly concentrated in the sarcolemma of the adult vertebrate neuromuscular junction. Accumulations of AChRs have also been demonstrated in extrajunctional regions of denervated muscle (29). Similarly, receptor accumulations have been found on both noninnervated and innervated muscle fibers grown in tissue culture (21, 25, 45). Some receptors are located (within the resolution of the techniques employed) precisely at sites of transmitter release (8, 23). The establishment of accumulations of receptors as a function of culture age has been studied (48) and suggestions as to how the accumulations develop have been made (2, 3), but the cellular and molecular mechanisms which regulate formation of the accumulations remain unknown. Ultrastructural approaches have been taken to obtain information on these mechanisms. Vogel and Daniels (47) used immunoperoxidase staining to visualize bound α-bungarotoxin (α-BGT, a ligand specific for the nicotinic AChR) at the electron microscope level. They concluded that patches of reaction product could not be correlated consistently with any particular membrane or submembrane structure. The freeze-fracture technique reveals a number of large angular intramembrane particles at the tops of postsynaptic junctional folds in mature amphibian (26) and mammalian synapses (40). These particles are located in the region which is highly sensitive to ACh and to which α-BGT is bound (19). We thought that by using the freeze-fracture technique on cultured muscle, we might be able to find a similar ultrastructural correlate of the AChR. We could then analyze the distribution of such structures at a resolution that might indicate how AChRs are organized in the sarcolemma, as well as give clues to the underlying molecular events responsible for the insertion, maintenance, and turnover of these receptors. The present study deals with the intramembrane structures revealed by freeze-fracture in specific regions of muscle fibers grown in culture. Before fracturing, these regions were labeled by the binding of α-bungarotoxin which had been coupled to a fluorescent probe, tetramethylrhodamine (TMR-α-BGT). Preliminary reports have appeared (9, 39). While this work was in progress, two other groups of workers demonstrated clusters of large angular particles in developing muscle fibers. Peng and Nakajima (36) suggested that the particles were AChRs on the basis of their resemblance to particles found in postsynaptic membranes of neuromuscular junctions. Yee et al. (50) claimed that, within technical limits of resolution, clusters of particles were located in the sarcolemma of cultured chick myotubes in the vicinity of regions that were especially sensitive to iontophoretically-applied acetylcholine (ACh).

MATERIALS AND METHODS

Culture

Cell cultures from dissociated pectoral muscles of 11-d chick embryos were prepared as previously described (20) and grown on collagen-coated glass coverslips (Gold Seal; Clay-Adams, Parsippany, N. J.). To prepare for freeze-fracture, 3-mm-diameter circles were scored on the cover slips before coating with collagen. Cytosine arabinoside (10^{-5} M) was added for 48 h ~2 d after plating to eliminate fibroblasts. The culture medium was then renewed three times per week. A group of control cultures received no further treatment. In a second group of cultures, tetrodotoxin (TTX, 5×10^{-7} M) was added to the medium for 48–72 h at 2 d after plating. In a third group of cultures, explants of 14-d embryonic chick spinal cord were added at the edges of the scored circles. In these cultures, many muscle fibers became functionally innervated as indicated by spontaneous contractions (21, 23).

Mapping of α-Bungarotoxin Binding

Most of the liquid was removed from the culture coverslip, and its surface was covered with 50 μl of 10^{-7} M TMR-α-BGT in Eagle's Minimum Essential Medium to which either 1% horse serum or 2 mg/ml bovine serum albumin was added (MEM-protein). After 60 min, unbound toxin was removed by rinsing the coverslips 3–4 times for at least 10 min each in a large volume (>20 ml) of MEM-protein at 37°C in a humid 5% CO_2 atmosphere. Most cultures were then lightly fixed at 4°C for 30–60 min with 0.5–1% formaldehyde (freshly prepared from paraformaldehyde) dissolved in Eagle's MEM or in 0.15 M sodium cacodylate buffer, pH 7.4, and rinsed three times in cacodylate buffer containing 5% sucrose. However, some cultures were viewed in the living state. The scored circles were isolated by breaking away the remainder of the coverslips to yield areas for mapping and freeze-fracture.

Cultures were initially observed under Nomarski interference contrast optics, and the entire 3-mm-diameter areas were photographed through a ×6.3 objective (total magnification ×98.5). 5–10 selected fields were then photographed through a ×40 objective (NA 1.2; total magnification ×625) under Nomarski and epi-illumination fluorescence optics. For specific tetramethylrhoda-

mine fluorescence, Zeiss BP 546/9 and KP 600 excitation (Carl Zeiss, Inc., N. Y.) and Kodak 23A barrier filters were used. As a check for nonspecific fluorescence, a combination of filters designed for fluorescein isothiocyanate were used. Specimens were photographed on Kodak Tri-X film exposed for 1–4 min and push processed to ASA 1200 in Acufine developer (Acufine Inc., Chicago, Ill.). The low-magnification map of the culture was used to relocate regions of fibers having fluorescent spots that had been viewed at high magnification.

Freeze-Fracture

The photographed cultures were fixed in 2.5% glutaraldehyde in 0.15 M cacodylate buffer for 1 h at room temperature and rinsed with this buffer. The buffer was replaced at 10-min intervals by 11%, 22%, and finally 33% glycerol in H_2O, where the cultures remained for 1–2 h. Yee et al. (49, 50) freeze-fractured cultured myotubes using the Balzers' complementary replica device (Balzers AG, Leichtenstein). However, the method employed here more closely follows that described by Pauli et al. (35) for other cell types. Specimen carriers were the same diameter but 0.1 mm taller than those normally supplied. A drop of a solution containing 30% polyvinyl alcohol (Gelvatol 20–30, Monsanto Co., St. Louis, Mo.) and 30% glycerol in H_2O was placed on a specimen carrier. The coverslip and culture was removed from the glycerol solution; its back was dried, and it was inverted onto the drop of polyvinyl alcohol solution. The drop deformed slowly to cover the surface of the specimen carrier. The coverslip was adjusted to be parallel to the surface of the carrier, and the sandwich was frozen in liquid Freon-22 (maintained near its freezing point) and stored in liquid N_2. The frozen sandwich was inserted into the complementary replica device, and fractured and replicated at −119°C in a Balzers 360 M apparatus (Balzers Corp., Nashua, N. H.). The specimen carriers were then slowly immersed in H_2O; replicas floated off as the polyvinyl alcohol solution dissolved. Replicas attached to the collagen layer came off during cleaning in gradually increasing concentrations of sodium hypochlorite (1–25%; Purex Corp., Lakewood, Calif.) in cacodylate buffer. Comparing the low-power light-micrographic maps of the original cultures with the resulting replicas allowed us to cut out portions of the replicas containing areas previously identified by their fluorescence. These portions were picked up on Formvar-coated slot grids and examined in an AEI-802 electron microscope operated at 80 kV. As a further aid in locating specific areas for electron microscopy, light micrographs (×25) of the grids were taken using epi-illumination. This method allowed the replicas prepared from both leaflets of a given portion of membrane to be located on their respective grids.

Matching of Fluorescence with Membrane Features

Micrographs of replicas of muscle fibers were made at both high (×27,000 or 32,000) and low (×1,400) plate magnifications in areas coincident with previously mapped fluorescence. Boundaries were traced around clusters of 100-Å particles in high-magnification prints and an internegative was made. Reduction of this image to the size of the low-power micrographs allowed us to trace the boundaries onto these micrographs wherein particles themselves could not be seen. From the relative magnification factors, and by reference to features of the muscle fibers visible both in electron micrographs of the replicas and in Nomarski images, the low-power electron micrographs were reduced to the exact size of, and could be placed in exact register with, the fluorescence micrographs.

Quantitation

For particle counting, electron micrographs of replicas were made at a magnification of at least 70,000. Particles were counted by hand, while areas were measured with a digitizer attached to a Hewlett-Packard 9810A calculator.

RESULTS

Membrane Features

Essentially all of the muscle fibers in the sparse monolayer cultures were fractured, thus yielding complementary replicas of nearly 50% of the total surface membrane in the culture. Cross-fractures of muscle cytoplasm were obtained only rarely. Most of the fractures occurred in the membrane adjacent to the collagen layer, as shown by the predominance of external leaflets in replicas obtained from the coverslip side.

The corresponding cytoplasmic and external leaflets of a portion of a muscle fiber are shown in Figs. 1 and 2. The membrane was usually locally smooth but did have some larger-scale foldings similar to those seen with Nomarski optics. Microrippling of the cleaved surface, apparently due to slow freezing of the cultures, was occasionally seen. This artifact affected particularly the external leaflets (Figs. 2 and 6). These leaflets are adjacent to the glass coverslip through which heat transfer is slow compared to that through the copper specimen carrier. Several membrane structures were evident. Invaginations, appearing as pits 20–30 nm in diameter in the cytoplasmic leaflet or as "volcanoes" in the external leaflet, were found throughout the membrane. They occurred both singly and in small groups in which nearest neighbors were separated by a relatively constant distance (Fig. 3). Occasionally, membranes contained several hundred invaginations arranged in parallel

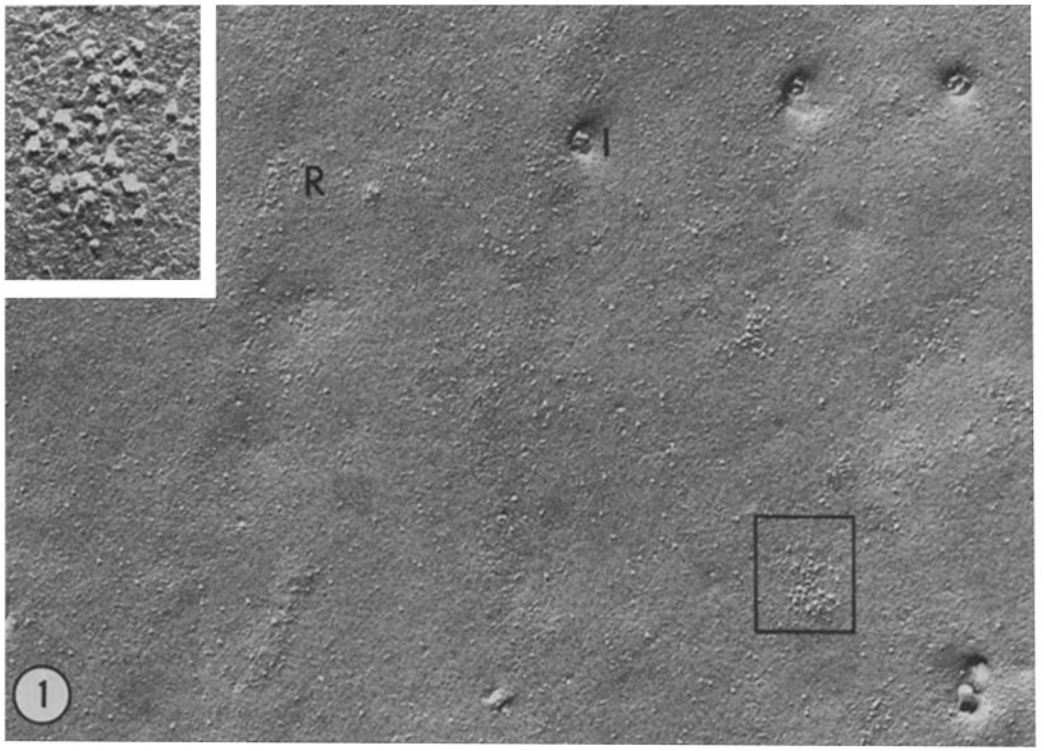

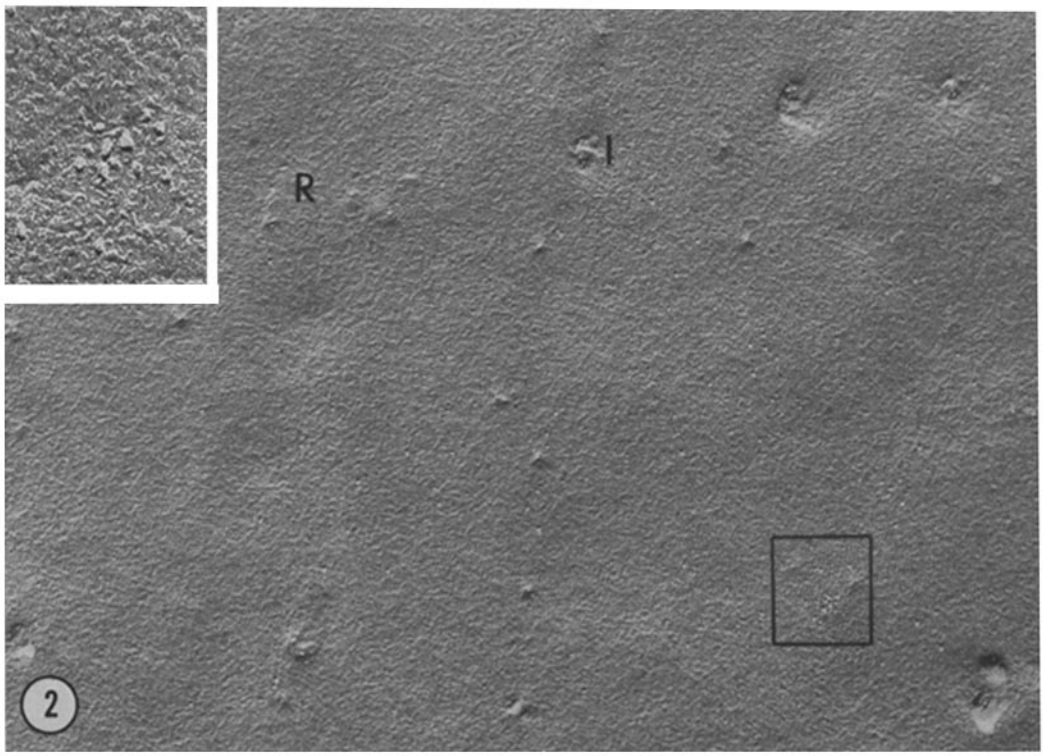

FIGURES 1 and 2 Complementary leaflets of a portion of sarcolemma from a myotube in a control culture. Fig. 1: cytoplasmic leaflet, Fig. 2: external leaflet. Due to the geometry of fracturing and replication, the shadowing with platinum is in opposite directions when the images are aligned. Therefore, in this and similar figures, the external leaflet should be viewed upside-down to observe particles with the proper perspective. Membrane features include: invaginations (*I*) 20–30 nm in diameter; round-topped, 70-Å Diam particles associated with ridges (*R*); and clusters of angular particles ~100 Å in diameter (circumscribed areas and insets). The particles appear to be similar in both cytoplasmic and external leaflets, but are more numerous in the cytoplasmic leaflets. The external leaflet has some micro-rippling, apparently an artifact of freezing (see Materials and Methods). Figs. 1 and 2, × 42,000; insets, × 130,000.

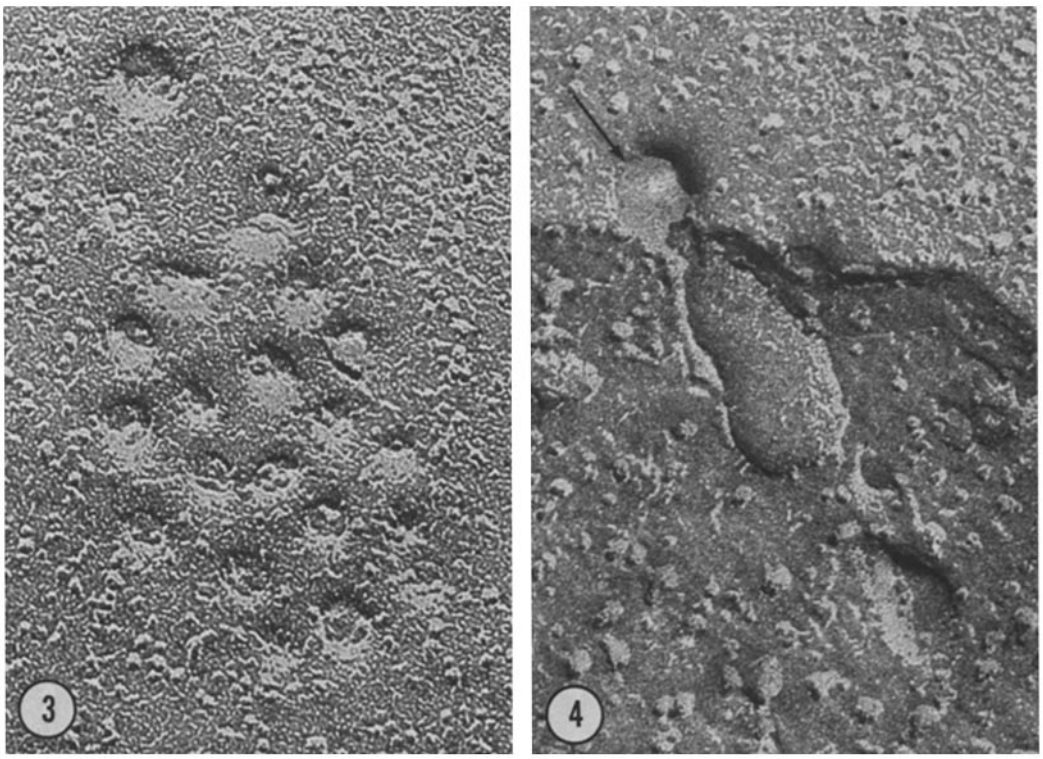

FIGURE 3 A group of invaginations in the cytoplasmic leaflet of a sarcolemma of a myotube from a control culture. The center-to-center distance between nearest neighbors is 71 ± 2 nm. The "bottoms" of the invaginations vary in appearance from that of cross-fractured ice to that of a smooth membrane. × 150,000.

FIGURE 4 A rare cross-fracture showing an invagination in the cytoplasmic leaflet related to a membrane-bounded tube extending into the sarcoplasm. × 180,000.

lines with a similar nearest neighbor distance. The distinctly-grouped distribution of these invaginations suggests that they are structurally if not functionally related to each other. Such invaginations may be the surface openings of the extensive tubulo-vesicular network (49) located beneath the surface of cultured chick skeletal muscle fibers (16, 22). Rare cross-fractures revealed that at least some invaginations were related to channels in the sarcoplasm (Fig. 4). Some invaginations may also be caveolae (36), present in both smooth (38) and skeletal muscles (14). Caveolae and T-tubule openings are found in close proximity to each other and are said to be indistinguishable in freeze-fracture replicas (24).

Several kinds of particles were found which we have grouped into three classes. Small (<50 Å Diam) particles were evenly distributed throughout the membrane. Their concentration was somewhat higher in cytoplasmic than in external leaflets. Somewhat larger (~70 Å Diam) round-topped particles were seen in the cytoplasmic leaflet, often associated with gentle ridges (Fig. 1). Neither of these classes of particles was studied systematically. We also found orthogonal assemblies of particles resembling the square arrays seen in adult rat muscle (40), but these occurred too rarely ($<0.1/mm^2$) for quantitative study as yet.

The largest particles (≥100 Å Diam) were angular, as judged by the shape of the shadows they cast, and were found in three arrangements in the sarcolemma: singly; as members of tightly-packed clusters containing 3–2,000 particles; and (in TTX-treated myotubes) in diffuse patches a few microns in diameter. A background level of 5–10 large particles per square micron was present throughout the sarcolemma. Clusters were readily recognizable. They consisted of a high and relatively

uniform concentration of large particles (3,500–4,000/μm^2) within an area defined by sharp borders at which the concentration dropped suddenly to the background level. Smaller clusters were nearly round but larger ones were often elongated (Fig. 5). These clusters were found in plasmalemmas of control and TTX-treated myotubes, and in myotubes from nerve-muscle co-cultures. Clusters were found both singly and in groups of three or more spaced <0.5 μm apart. Larger groups contained up to 15–20 clusters spaced as little as 20–30 nm apart. The diffuse patches seen with TTX treatment contained some clusters, particularly at or near their borders. Otherwise, the large particles were spread over the patch at a concentration of 1,000–1,500/μm^2, rather than occurring as a number of distinct clusters.

Within the clusters, many, but not all, of the particles cast platinum shadows which were distinctively triangular or diamond shaped (Figs. 1, 2, 5, 6, 24, 25, 28). The heterogeneous appearance may be due to similar particles having different orientations. It is not clear whether these different orientations reflect the situation in the living membrane or whether they are an artifact of fixation or fracturing. Alternatively, the clusters may indeed contain smaller, more spherical, particles in addition to the large angular particles just described.

The complementary replica technique allowed us to look at areas of external leaflets of membranes which were directly apposed to areas of the cytoplasmic leaflet having clusters of large angular particles. Such areas of external leaflets also had large particles (insets of Figs. 1 and 2). Particles in the external leaflets were indistinguishable from those appearing in the apposing cytoplasmic leaflets but were present in lower concentration. The ratio of the number of particles on the external leaflet to the number of particles on the cytoplasmic leaflet was ~0.5–0.6 to 1, but there was great variation between individual clusters. The ratio was not markedly altered by binding of bungarotoxin, nor was there a large difference in distribution of particles at points of nerve-muscle contact. No pits were seen in either leaflet corresponding to a large particle in the opposing leaflet although pits complementary to particles did occur in the membranes of adjacent nerves.

With respect to their size, shape, variability in appearance, close aggregation, and predominance in the cytoplasmic leaflet, the large angular particles resembled those seen in postsynaptic membranes of neuromuscular junctions of both frog (28, 37) and rat (15, 40). Since they appear in areas known to bind α-bungarotoxin (19) and to be sensitive to acetylcholine, these particles have been imputed to be acetylcholine receptors (40, 41).

Association of α-Bungarotoxin Binding with Large Particles

To gain further evidence on the relationship between membrane features and nicotinic acetylcholine receptors, we mapped the distribution of binding sites for the specific ligand α-bungarotoxin coupled to the fluorescent probe tetramethylrhodamine (TMR-α-BGT). Fluorescent spots were found on the lower surfaces of myotubes, adjacent to the collagen substrate, as well as on the upper free surfaces (2, 30).

To assure that the spots we observed were due to the specific binding of TMR-α-BGT, several experiments were performed. Muscle fibers to which no TMR-α-BGT was bound did not show TMR-specific fluorescence. A saturating dose of unlabeled toxin bound before exposure to labeled toxin also inhibited TMR-specific fluorescence. Occasionally, the same intense spots were seen when viewing with filter combinations designated for fluorescence due to either rhodamine or fluorescein. Such spots were usually associated with highly refractile cell organelles or debris and were considered nonspecific. Both living and fixed cells had similar patterns of fluorescent spots, but the latter sometimes had slightly higher background fluorescence. Apparently, TMR-α-BGT does not change the distribution of particles since we found similar patterns of patches and clusters on control, innervated, and TTX-treated muscle fibers which had never been exposed to the toxin (Cohen and Pumplin, unpublished observations; cf. references 36, 50).

Freeze-fracture replicas of areas of membrane having intense TMR-specific fluorescence were examined as described in Materials and Methods. Patches of membrane containing large angular particles were invariably found to coincide with fluorescent spots (Figs. 8–11, 15–16, and 18–19). In addition, variations in concentration of particles within a patch were reflected as variations in fluorescence in the spot. In a few cases no particles were found where fluorescence indicated they should be (Figs. 8–9). These occurred in thin areas of muscle fibers where it was impossible to tell by light microscopy whether the fluorescence was associated with the upper or lower surface. We

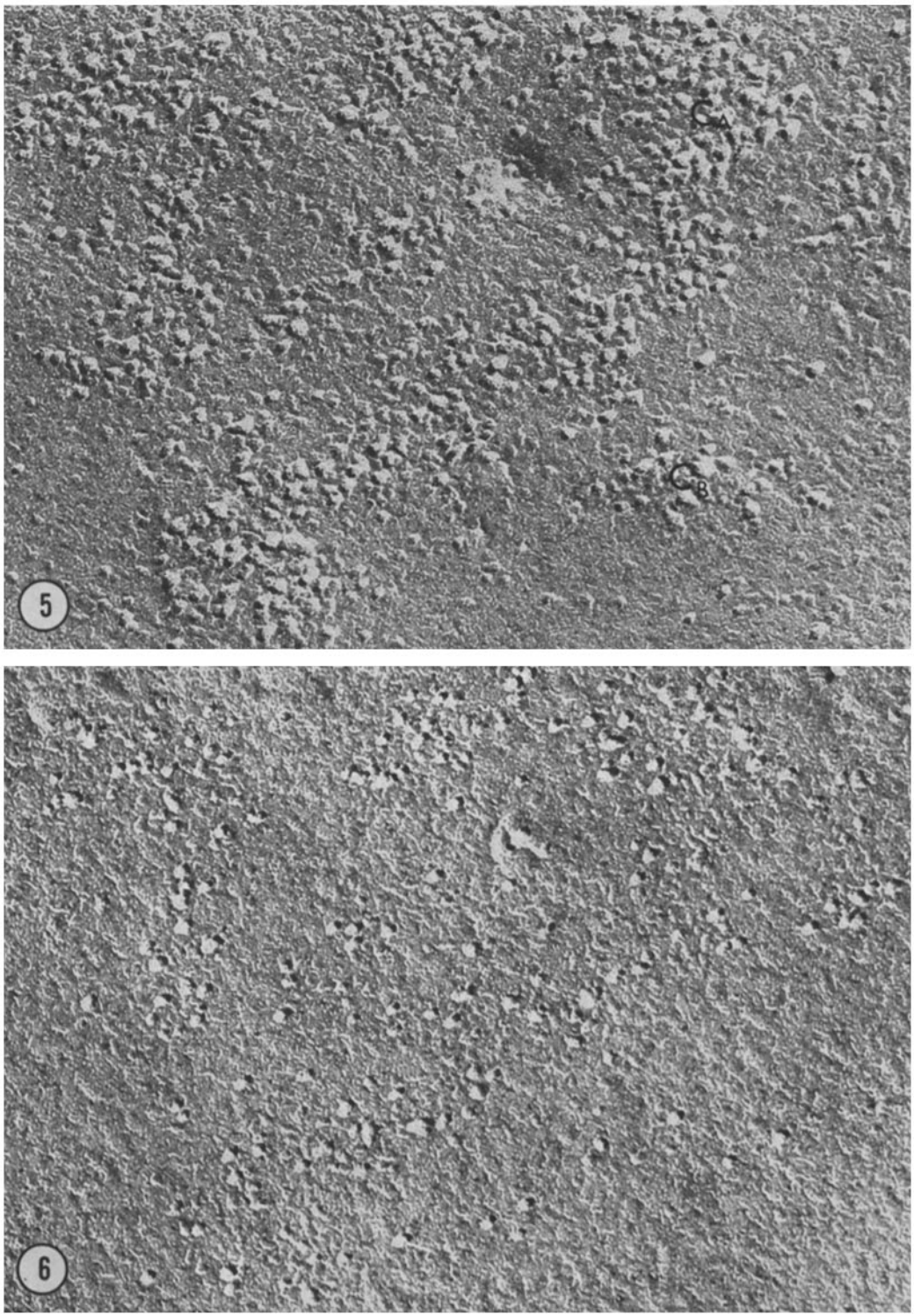

FIGURES 5 and 6 Complementary views of a small portion of a patch of grouped clusters in the sarcolemma of a myotube from a control culture. Note the variations in size and shape of clusters C_A and C_B and the presence of large particles in the external leaflet (Fig. 6) in areas coextensive with the clusters in the cytoplasmic leaflet (Fig. 5). Clusters were circumscribed on micrographs of cytoplasmic leaflets at this magnification, and were then photographically reduced to allow comparisons with fluorescence. The area in these figures is indicated by the arrow in Fig. 9. Figs. 5 and 6, × 150,000.

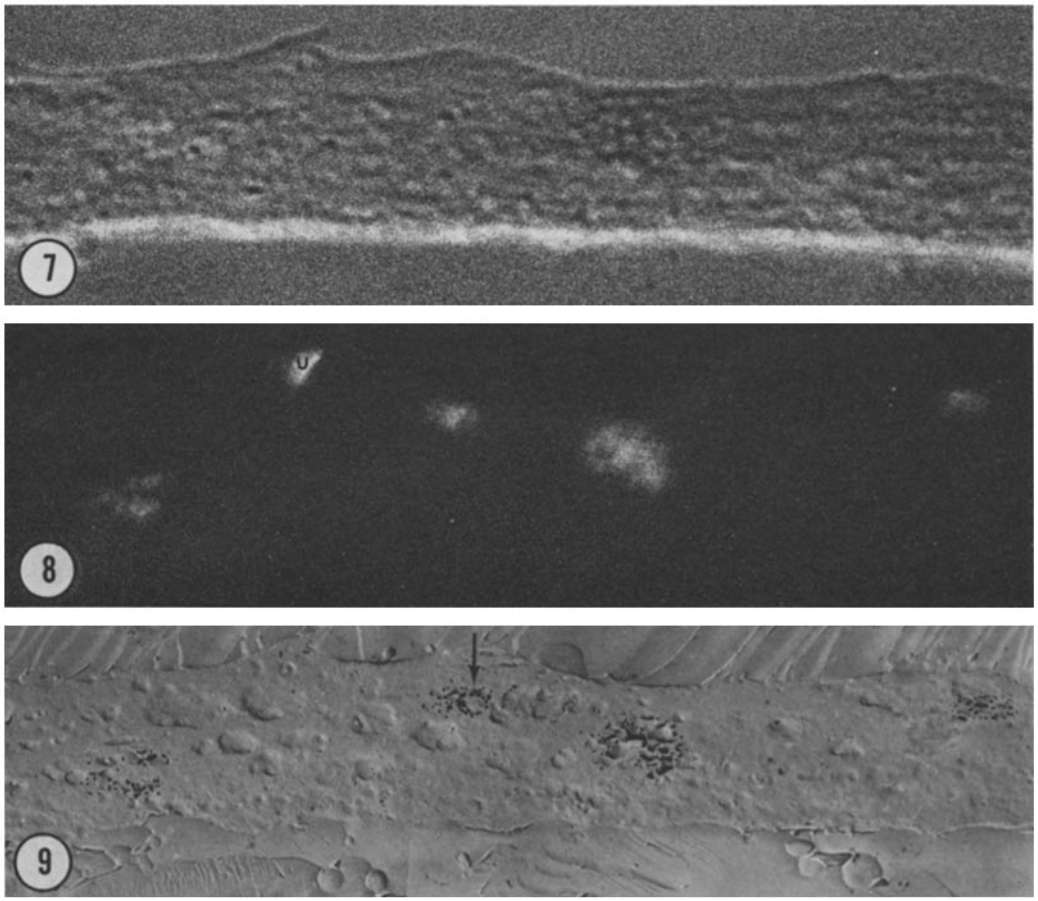

FIGURES 7–9 A portion of a muscle fiber from a control culture as viewed by Nomarski optics focussed on the fiber's lower surface (Fig. 7), by tetramethylrhodamine fluorescence (Fig. 8), and by electron microscopy of the cytoplasmic leaflet of the sarcolemma of this surface of the fiber (Fig. 9). All views are at the same magnification and have been placed in register. The correspondence between the boundaries of the fiber in Figs. 7 and 9 shows that the fiber was relatively flat. Note the good agreement between the locations of α-bungarotoxin binding (fluorescent spots, Fig. 8) and of clusters of large angular particles (dark patches, Fig. 9). No cluster corresponds to the fluorescent spot marked *u*. We believe that this resulted from binding of α-BGT to the upper surface of the myotube whereas the lower surface, next to the cover slip, was fractured. The arrow in Fig. 9 indicates the clusters shown in Figs. 5 and 6. Figs. 7–9, × 2,000.

assumed that fluorescence was due to toxin bound on the upper surface of the fiber while the lower surface was fractured.

This exact correspondence between the locations of patches of large angular particles and fluorescence due to bound α-bungarotoxin was observed in untreated control cultures (Figs. 8–9), in cultures treated with tetrodotoxin (Figs. 10–11), and on both innervated (Figs. 18–19) and noninnervated (Figs. 15–16) fibers in co-cultures of muscle and spinal cord explants. Differences in the appearance of such patches under various treatments are described below.

Control Cultures

Relatively few spots of fluorescence were found on 6- to 10-d-old myotubes in control cultures; many fibers had no intensely fluorescent areas at all. Fluorescent spots were small (1–2 μm). Spots on the lower surface were about evenly divided between the center and periphery of the fibers. Often they were found at peripheral bulges in the

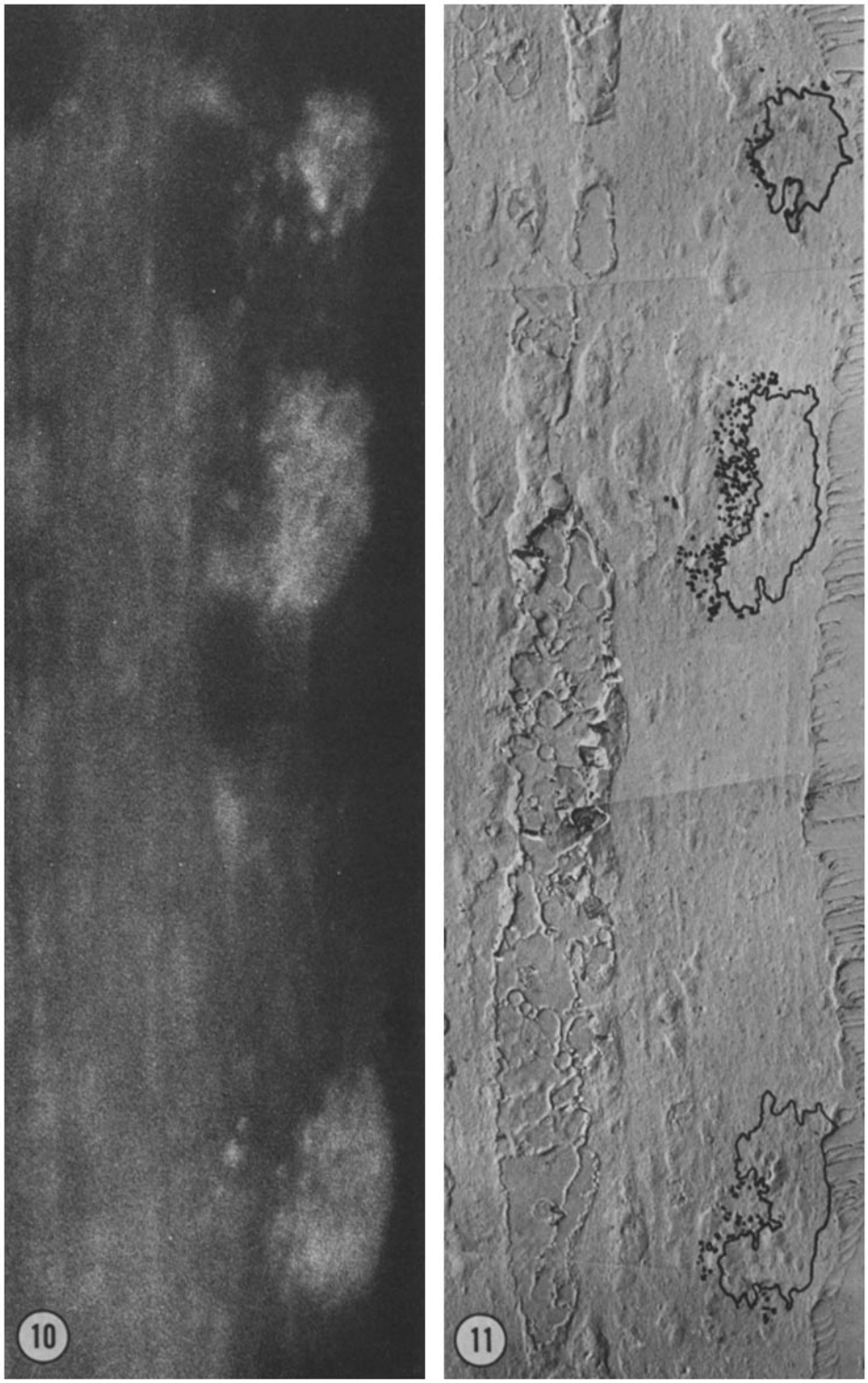

FIGURES 10 and 11 Portion of a myotube from a culture grown in the presence of 5×10^{-7} M tetrodotoxin. Fluorescent spots due to binding of TMR-α-BGT (Fig. 10) corresponded with patches of particles outlined on the freeze-fracture replica (Fig. 11). The patches of particles were larger on myotubes treated with TTX than on control myotubes. Treatment with TTX also resulted in patches with many smaller adjacent clusters (middle patch, Fig. 11). Background fluorescence appeared as streaks (Fig. 10), for which there was no corresponding feature in freeze-fracture replicas of the sarcolemma. Figs. 10 and 11, × 2,100.

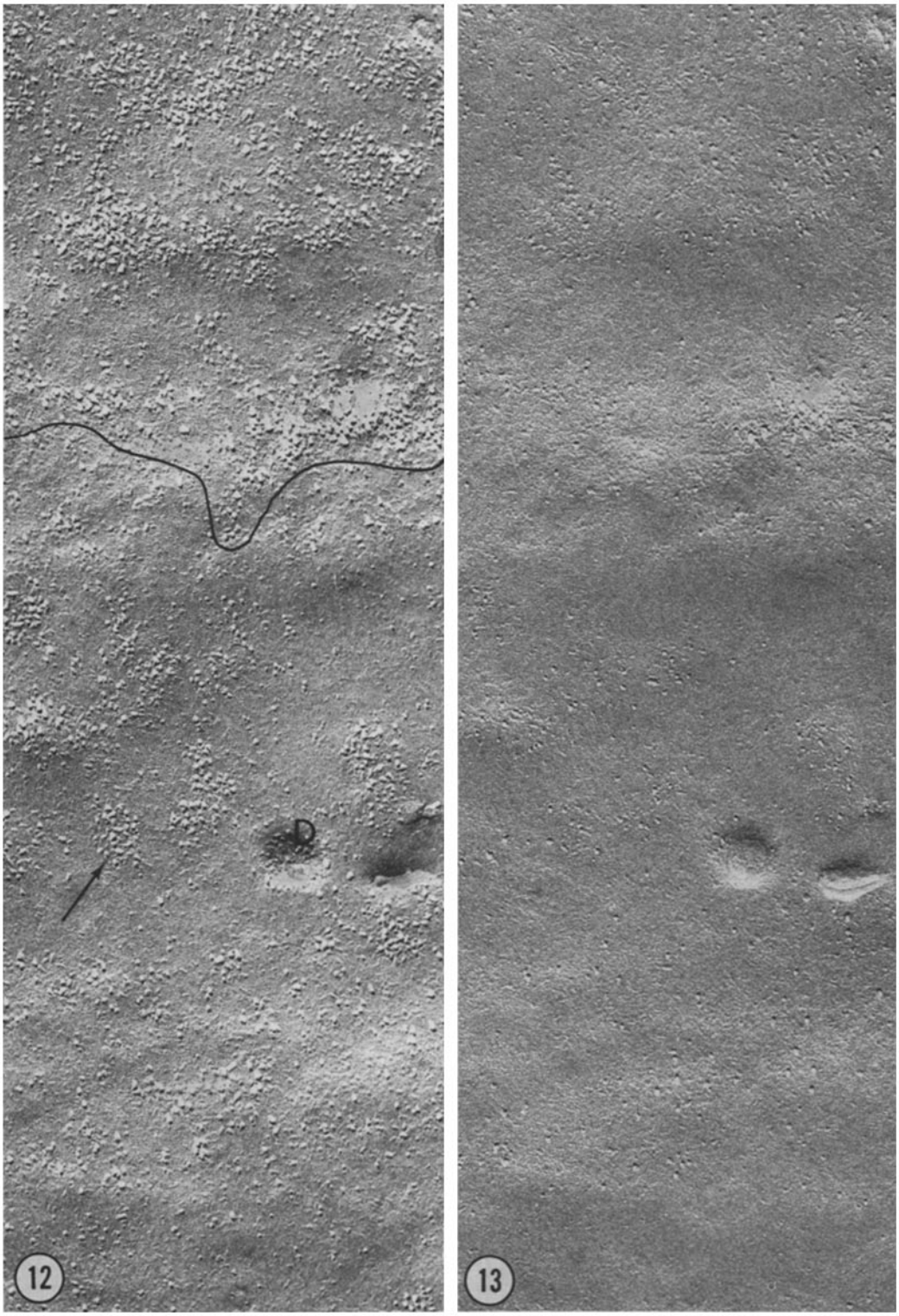

FIGURES 12 and 13 Complementary high power views of a portion of the edge of a large patch of particles found in the sarcolemma of a myotube grown in the presence of 5×10^{-7} M tetrodotoxin. This myotube was in a different culture than the one shown in Figs. 10 and 11. The line indicates the probable boundary of the patch (more easily determined from lower magnification micrographs, as were used for the outlines shown in Fig. 11). Outside the patch (below the line) there are several clusters (single arrow) of 100-Å angular particles and a large depression (115 nm Diam) also containing particles (*D*). Although particles are less numerous in the external leaflet (Fig. 13), their distribution follows that of the particles in the cytoplasmic leaflet. Figs. 12 and 13, × 74,000.

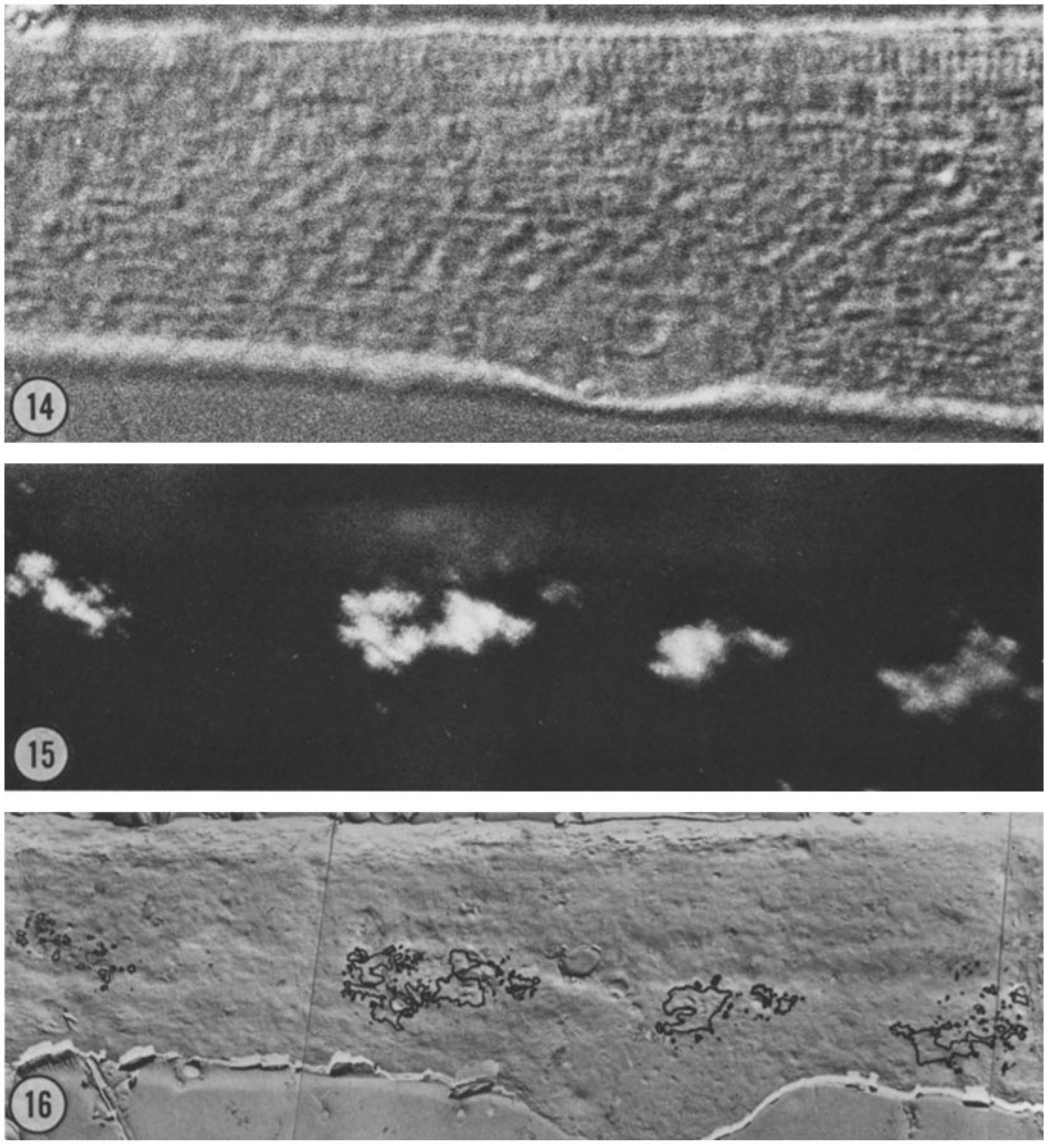

FIGURES 14–16 A myotube from a coculture of myotubes with spinal cord explants as viewed by Nomarski optics (Fig. 14), fluorescence of TMR-α-BGT (Fig. 15), and freeze-fracture replication of the lower surface (Fig. 16). All micrographs have the same magnification and were placed in register. Fluorescent spots due to binding of α-bungarotoxin (white areas in Fig. 15) corresponded well with patches of particles in the sarcolemma (dark spots and outlined areas in Fig. 16). The patches shown were not associated with regions of nerve-muscle contact and, conversely, nerve-muscle contacts occurred on this fiber without patches of particles or α-bungarotoxin binding. Figs. 14–16, × 2,200.

fibers, some bulges being associated with hypolemmal nuclei (21). At the electron microscope level, the patches were composed of large angular particles arranged in distinct clusters in close proximity to one another (Figs. 5 and 9).

TTX-Treated Cultures

At least one intensely fluorescent spot was invariably found on 6- to 10-d-old myotubes grown in the presence of 5×10^{-7} M TTX for 48–72 h

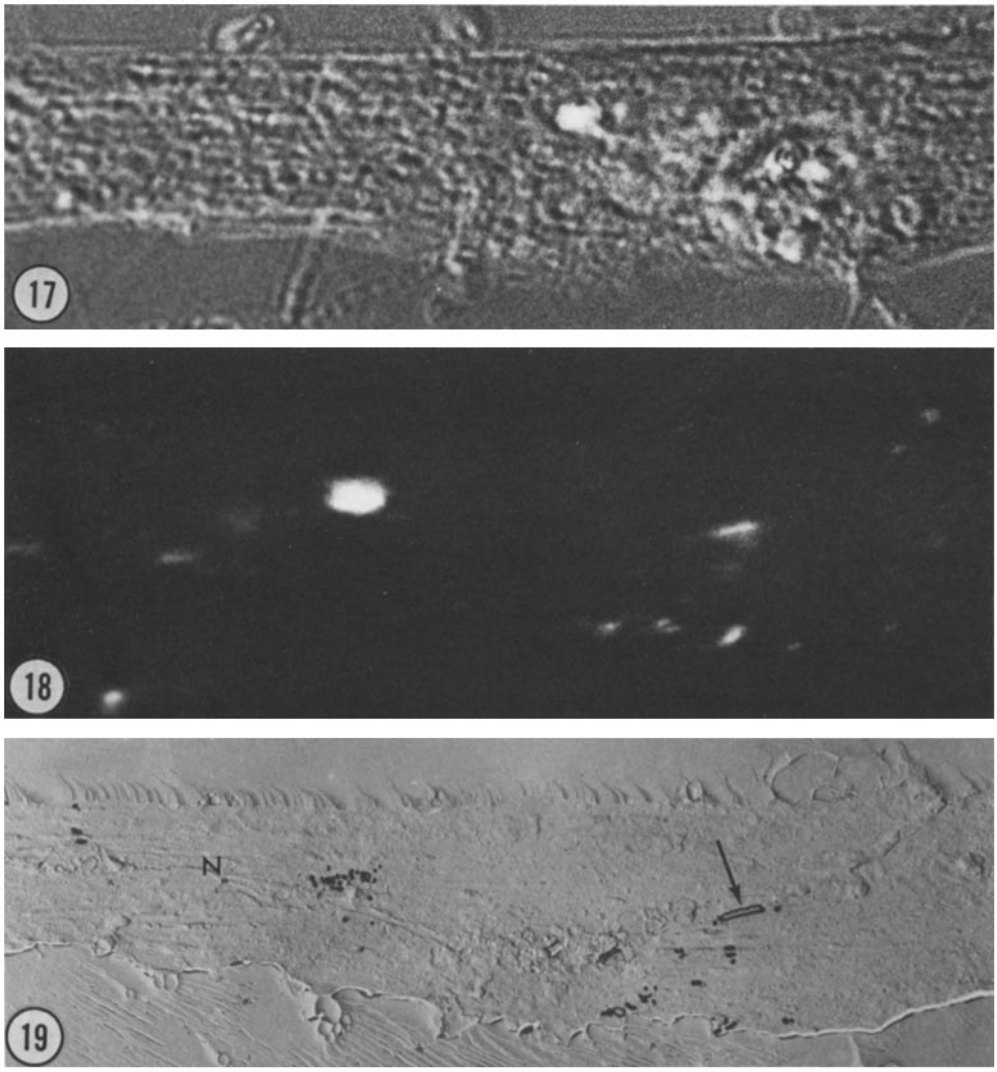

FIGURES 17–19 A muscle fiber from a coculture of myotubes with spinal cord explants as viewed by Nomarski optics (Fig. 17), fluorescence of TMR-α-BGT (Fig. 18), and freeze-fracture replication of the lower surface (Fig. 19). All micrographs have the same magnification and were placed in register. Fluorescent spots due to binding of α-bungarotoxin (white areas in Fig. 18) corresponded well with patches of particles in the sarcolemma (dark spots and outlined areas in Fig. 19). A nerve fiber (*N*) coursing over the surface of the muscle can be seen as an irregular channel. Patches of particles and fluorescence occurred adjacent to portions of nerve-muscle contacts (arrow, Fig. 19) as well as away from such contacts. A portion of the nerve-muscle contact indicated by the arrow is shown in Fig. 25. Figs. 17–19, × 2,000.

(Fig. 10). These patches were larger than those seen in control myotubes. Many myotubes had hazy longitudinal streaks of fluorescence covering large areas of the sarcolemma; small (<0.2 μm Diam) bright spots often punctuated the hazy areas (Fig. 10).

Patches of large angular particles in freeze-fracture replicas were coextensive with spots of intense fluorescence, and variations in particle concentration within the patches were reflected as variations in fluorescence intensity (Figs. 10 and 11). Complementary membrane leaflets of a portion of such

a patch are shown in Figs. 12 and 13. Areas of high concentration of large angular particles had well-defined boundaries in myotubes grown in TTX. However, the organization of these areas was somewhat different from that seen in control or innervated myotubes. Specifically, in membranes of myotubes treated with TTX, the patches had a higher concentration of particles than background areas and possessed a corona of smaller clusters with a yet higher concentration of particles (lower portions of Figs. 12 and 13). Smaller clusters are indicated by the small circles at the periphery of the patches in Fig. 11. The boundary between smaller surrounding clusters and the "main" patch was tortuous and at times difficult to ascertain. In addition, the main patch often contained areas with high concentrations of particles (comparable to those in the peripheral clusters) as well as "islands" in which large particles were scarce. These islands did contain smaller particles and were at times visible as areas of decreased TMR-α-BGT fluorescence in living, unfixed cultures, suggesting that the islands are not fixation artifacts.

Clusters of particles were not always found to coincide with the small bright spots punctuating hazy areas of fluorescence. The fluorescence may result from toxin bound to or trapped within the subsurface tubulovesicular network, although it is difficult to see why this phenomenon should occur preferentially in TTX-treated cultures.

Nerve-Muscle Co-Cultures

In co-cultures of muscle cells and spinal cord explants, some myotubes, contacted by neurites, were seen to contract rapidly, synchronously, and repetitively. These were identified as innervated, since under these conditions synaptic potentials can always be recorded with an intracellular microelectrode (8). Fluorescent spots on such myotubes were generally brighter, larger, and sometimes more elongated than those on noninnervated myotubes in the same culture or in sister cultures. Many of these spots were adjacent to neurites coursing over or along the surface of the myotube. These neurites could be readily identified both with Nomarski optics and in freeze-fracture replicas.

Clusters of large angular particles were also coextensive with fluorescent spots on innervated myotubes. Matched fluorescence and clusters were found both away from (Figs. 14–16) and adjacent to (Figs. 12–19) appositions between neurites and myotubes. Some neurites crossed muscles but neither fluorescence nor clusters of particles were found along the appositions. In other cases, both the fluorescent patch and the cluster of particles were confined to short segments along the nerve fiber (Figs. 17–19). The large angular particles were visible in a narrow ($\leq$0.5 mm) band of the sarcolemma extending alongside the nerve. In some nerve-muscle contacts, the band of particles was continuous; in others, the band was divided into smaller clusters by particle-free areas which tended to be perpendicular to the long axis of the nerve.

Some neurites ran in small grooves in the surface of the muscle; fractures then split the portion of the nerve membrane opposite that immediately apposed to the myotube (Fig. 25). A more favorable case, in which we obtained complementary replicas of the neuronal plasmalemma directly apposing the muscle, is shown in Figs. 22 and 23. The nerve was identified by Nomarski optics (Fig. 20), and a coextensive patch of fluorescence was present (Fig. 21). Large angular particles were concentrated in the membrane of the myotube both at the sides of and (judging by the fluorescence) within the contact area between nerve and muscle. In addition, in a few cases the cytoplasmic leaflet of the nerve showed possible specializations, i.e., vaguely linear aggregates of large particles which were associated with clusters of 100-Å particles in the corresponding cytoplasmic leaflet of the muscle. These aggregates were absent from the neuronal plasmalemma which did not directly appose the muscle (Fig. 25). The aggregates were also absent if there were no clusters of receptor particles in the apposing sarcolemma. These aggregates of particles may be a form of presynaptic specialization or a precursor thereof, but this is only speculative without freeze-fracture descriptions of presynaptic specializations of chick neuromuscular junctions.

Large Angular Particles Associated with Sarcolemmal Depressions

Infrequently, we found clusters of 10–25 large angular particles within shallow sarcolemmal depressions ~110 nm in diameter. These were more often seen on muscle fibers grown in the presence of TTX (Fig. 28) but were also found on control and innervated fibers. The depressions often appeared in the vicinity of (Figs. 12 and 26) and immediately adjacent to (Fig. 28) existing clusters.

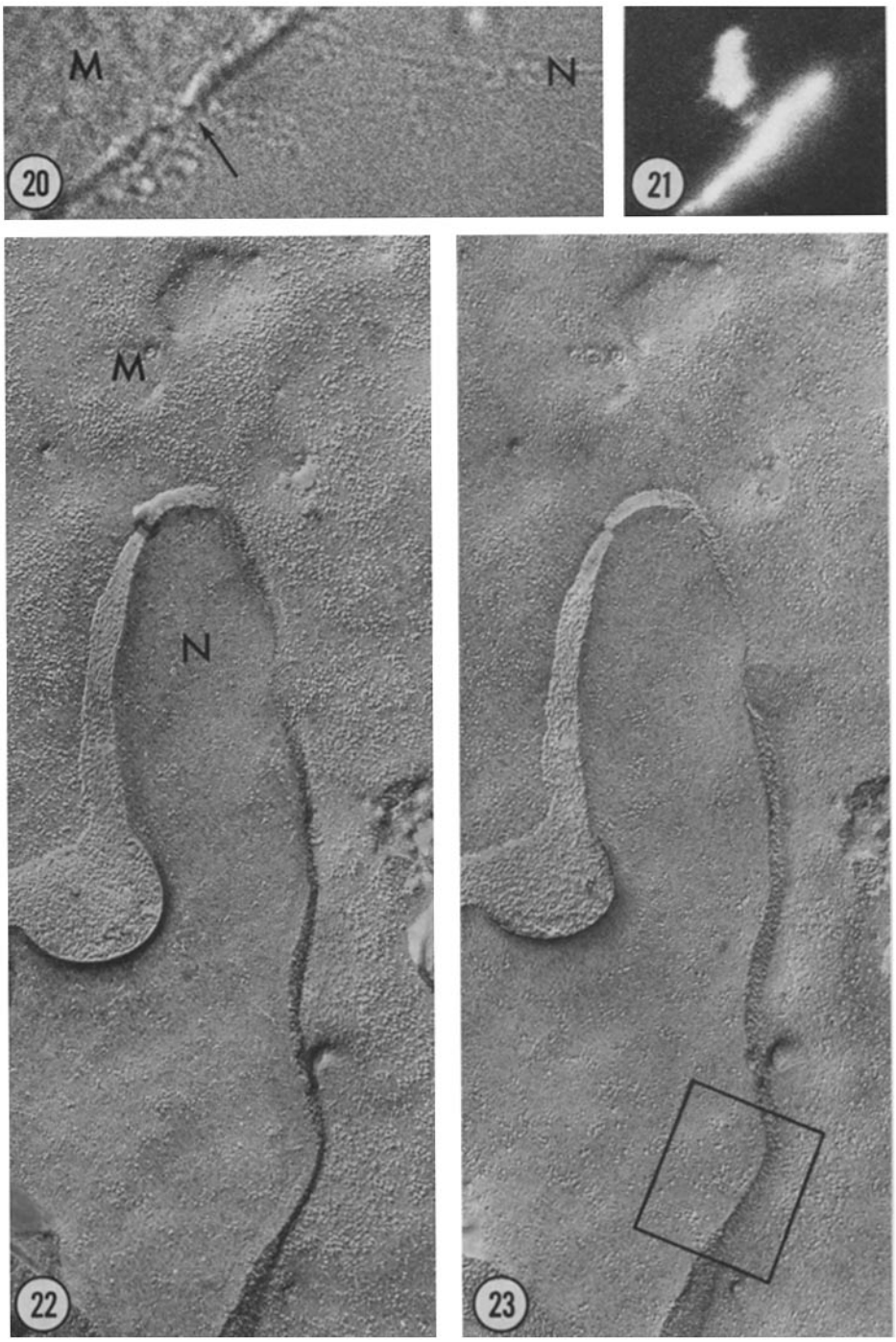

FIGURES 20–23 Four views of a nerve-muscle contact. With Nomarski optics, the nerve (*N*, Fig. 20) can be seen to approach the myotube (*M*) and contact its lower surface beginning at the arrow. The contact area is marked by intense fluorescence due to bound TMR-α-BGT (vertical patch, Fig. 21). Additional fluorescence following the edge of the myotube is due to debris, as it also appeared when filters for fluorescence due to fluorescein were used (not shown). Figs. 22 and 23 are complementary replicas of the contact area. Fig. 22 shows the cytoplasmic leaflet of the sarcolemma (*M*) and the external leaflet of the neuronal plasmalemma (*N*), while Fig. 23 shows the external leaflet of the sarcolemma and the cytoplasmic leaflet of the neuronal plasmalemma. Large angular particles are concentrated in the sarcolemma adjacent to the nerve coextensive with the location of specific fluorescence. These particles occur in both leaflets. Possible specializations of the nerve plasmalemma (circumscribed area of Fig. 23) are shown enlarged in Fig. 24. Figs. 20–21, × 2,100. Figs. 23–24, × 46,000.

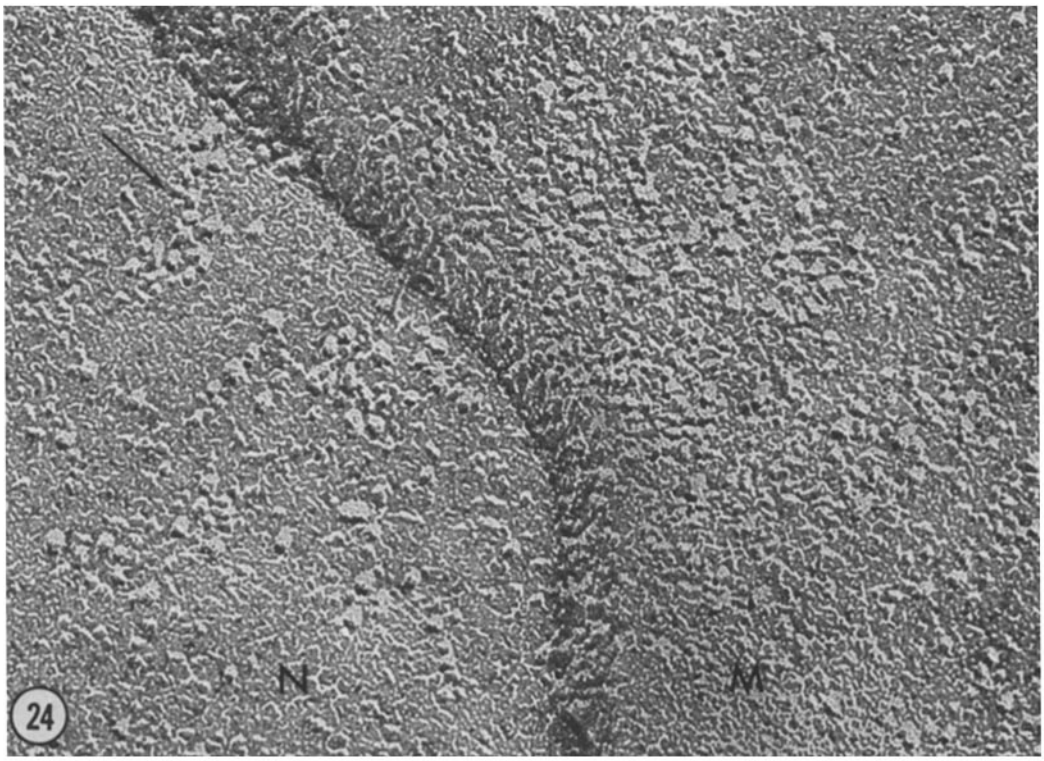
N
M
24

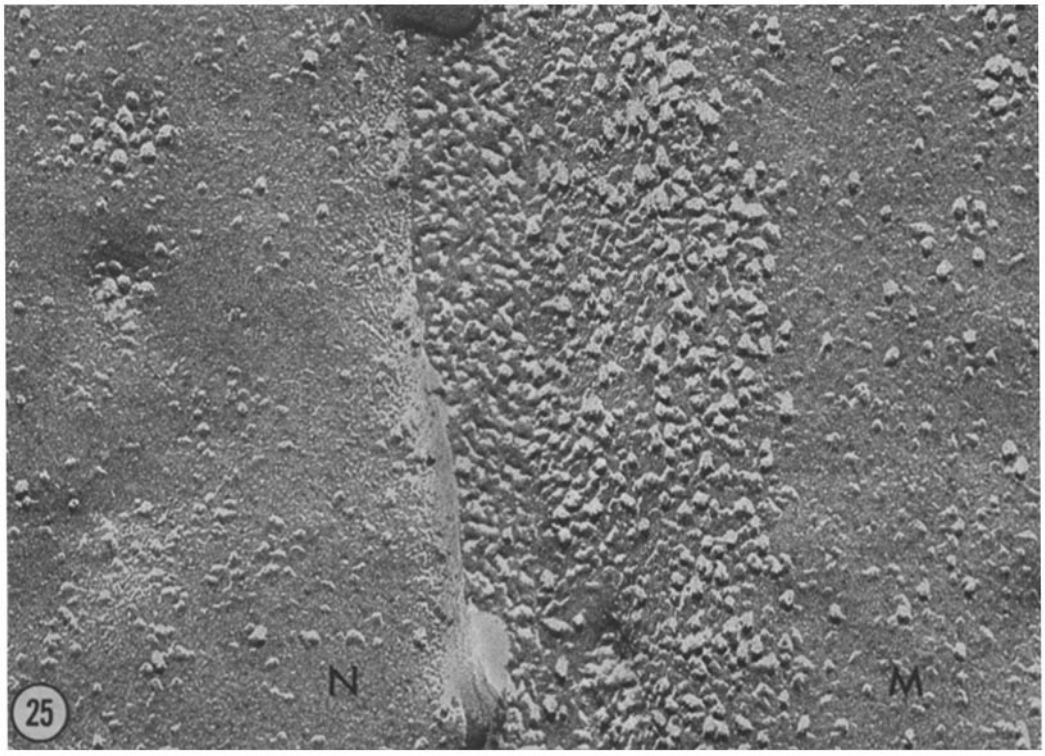
N
M
25

We believe that such deformations of the sarcolemma are transient structures which have been caught by fixation and, if so, represent a stage either in the merger of a membrane-bounded vesicle with the sarcolemma or the formation of a vesicle from a portion of the surface membrane. By this means, the membrane-associated particles could be added to, or withdrawn from, the sarcolemma. Whatever the direction of movement, the process involves a group of particles, rather than individual particles, associated with a depression of uniform size. We also found a single example (cross-fractures are uncommon in our system) of what may be a portion of a vesicle lying within the sarcoplasm (Fig. 27) which contains particles similar to those appearing in the shallow depressions and in clusters. The existence of such vesicles must be confirmed by a combination of thin-section and freeze-fracture techniques, however, since sarcotubular membranes also contain large particles at a relatively high concentration (10).

Gap Junctions

Fischbach (20), using a culture system similar to ours, found three examples of electrical coupling between nerve somas and muscle fibers. The significance of this infrequent finding is unclear. Since in other systems the suggestion has been made that electrical synapses are mediated by gap junctions (5) which have a characteristic freeze-fracture image (32), we made a preliminary search for these structures in our cultures. In no case were clear gap junctions demonstrable, but a more extensive, systematic investigation is underway to determine whether these structures do exist at some stage of synapse development.

DISCUSSION

Patches of large angular particles within the membranes of cultured skeletal muscle fibers were found to correspond precisely to areas of intense fluorescence due to bound TMR-α-BGT. Since no other structure was obviously more numerous in these areas and since the acetylcholine receptor is thought to span the membrane, this strongly suggests that these particles are the ultrastructural correlate of the AChR. Thus, intensely fluorescent patches truly reflect an increased concentration of receptors in the membrane and are not due to membrane folding. This finding agrees with those of Vogel and Daniels (47). The folds they depicted were of the order of several tenths of a micron in size, and they recognized that the reaction product itself obscured some specializations smaller than ~0.1 μm. Since the freeze-fracture technique is not limited by this difficulty, it is clear that the much smaller (25 nm) invaginations (c.f., Fig. 3) are not necessary to account for clustering of receptors.

The possibility exists that clusters are induced by external influences such as binding of α-BGT or chemical fixation. Although we did not determine the precise distribution of the cluster sizes in muscle fibers not exposed to α-BGT, clusters were qualitatively the same on such muscle fibers (Cohen and Pumplin, unpublished observations; references 36, 50). It is also unlikely that fixation with aldehydes induced clusters since particles elsewhere on the fibers remained dispersed. Fixation by rapid freezing might help clarify this point.

Heterogeneity of Particles

Heterogeneity may be introduced by different orientations of the particles in the membrane. Rash and Ellisman (40) suggested, for postsynaptic particles in mature synapses, that each particle consists of more than one receptor. The diversity of particle shapes on these relatively immature myotubes, if it exists in the living membrane, may

FIGURE 24 A nerve-muscle contact showing the cytoplasmic leaflet of the nerve (*N*) and the external leaflet of the muscle (*M*). The area circumscribed in Fig. 23 was turned right-for-left and magnified to ease visualization of the particles. Vaguely linear aggregates of large particles (arrows) appear in the cytoplasmic leaflet of the nerve membrane (*N*) apposed to the muscle membrane (*M*), in turn containing patches of putative receptor particles. × 180,000.

FIGURE 25 A nerve-muscle contact showing cytoplasmic leaflets of both nerve (*N*) and muscle (*M*). This arrangement of leaflets indicates that the nerve was partially embedded in a groove of the muscle surface and that the neuronal plasmalemma not immediately apposed to the muscle was fractured. Although large angular particles are in the sarcoplasm adjacent to the nerve in this location, there are no linear aggregates of large particles in the nerve membrane. This figure is a portion of the nerve-muscle contact indicated by the arrow in Fig. 19. × 180,000.

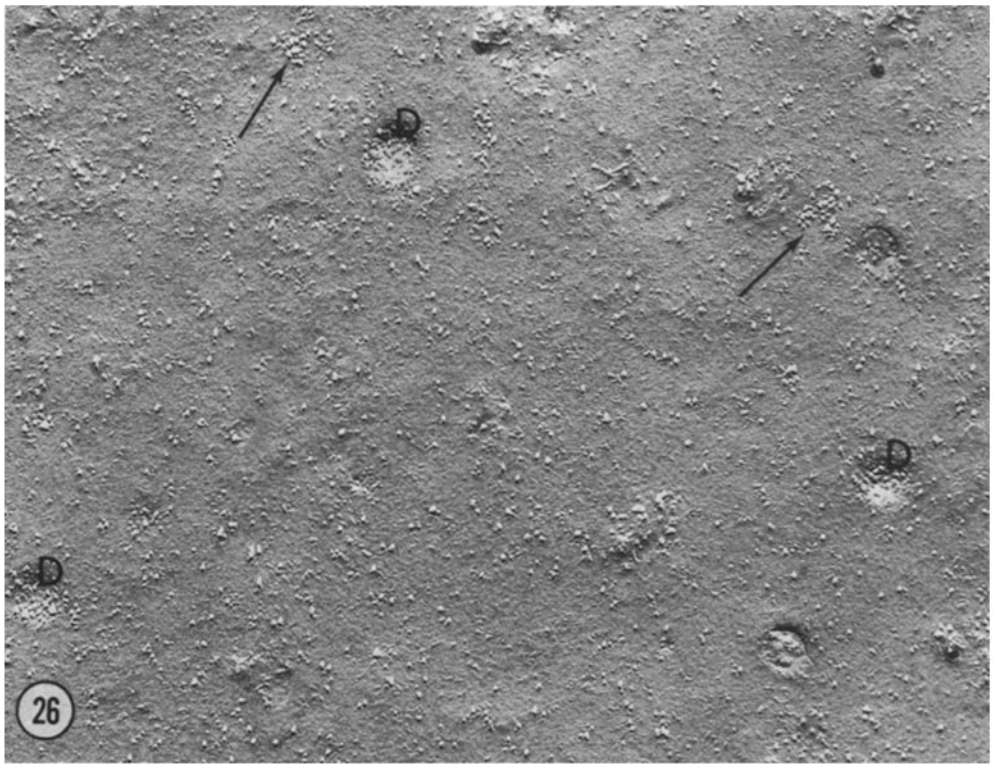
D
D
D
D
26


V
S
27

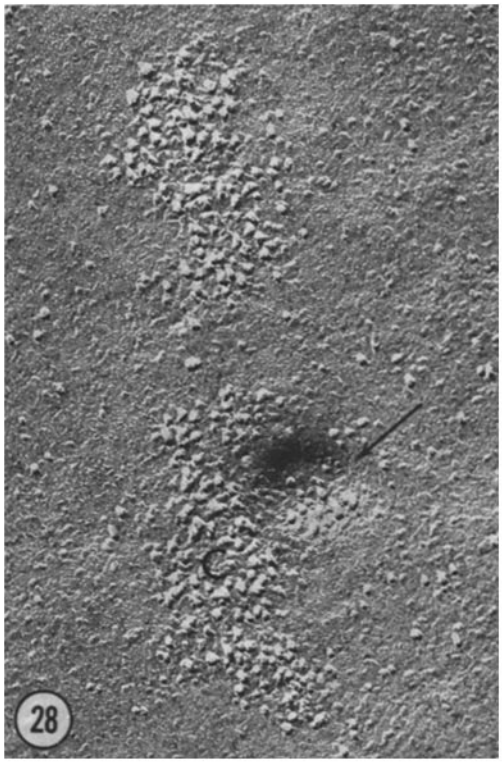
C
28

reflect a developmental stage in which the number of AChR associated as one particle is especially variable. Alternatively, the clusters of particles may include proteins other than AChR.

Some of the particles might represent the site of insertion of a cytoskeletal system. Arguing against this possibility is the absence in noninnervated myotubes of any obvious submembrane structure (47), although filamentous material does exist subjacent to postjunctional membranes (15).

Particle and Receptor Concentrations

The large angular particles on noninnervated myotubes are packed into discrete clusters at concentrations of 3,500–4,000/μm^2. However, clusters occupy only about one-half of the membrane area within the 1- to 5-μm diameter patches. Thus, the net density of particles over the entire patch was closer to 2,000/μm^2. If we use the approximation that one particle represents eight receptors (41), this means that AChRs in patches are packed at ~16,000/μm^2 which compares favorably with the value most recently determined by ^{125}I-α-BGT autoradiography (31).

In a similar fashion, we can reconcile our observations of nerve-muscle contacts with those of Betz and Osborne (6). These workers observed electrophysiologically that some "hot spots" at nerve-muscle contacts were more sensitive to ACh but were no larger in area than hot spots occurring away from such contacts. They suggested that this was due to a higher density of receptors at the contacts. Freeze-fracture reveals that hot spots, or patches, are composed of clusters of tightly-packed particles. The clusters are grouped together, but separated by areas of membrane with only a background concentration of the large particles. At points of nerve-muscle contact, the concentration of particles within the clusters is the same as that of clusters found elsewhere, but a greater proportion of the area of a patch is occupied by the clusters, thereby increasing the overall concentration of particles in the patch. The clusters themselves are also slightly larger at points of nerve-muscle contact (see Appendix). Both the fluorescence images and the freeze-fracture replicas show that many of the patches are not circular and that the patches are generally smaller (1–2 μm) than the hot spots reported by Betz and Osborne (5–10 μm) (6). The discrepancy in size may be due to the different systems used, ages of the cultures, conditions of growth, or the relative imprecision of the iontophoretic technique.

Neuromuscular Junctions

The presynaptic ultrastructure of the adult neuromuscular junction as revealed by freeze-fracture has been described by several investigators (references 1, 28, 40; for a review, see reference 27). Double rows of large particles usually associated with ridges have been described in the cytoplasmic leaflet of the neuronal plasmalemma. Since deformations presumed to be fusion sites of synaptic vesicles are found adjacent to these rows under suitable conditions of stimulation, it has been suggested that the rows of particles are related to the active zones of transmitter release. Many nerve-muscle contacts in our cultures had no particle specializations in either membrane. However, in a number of cases, we have seen discrete areas where large particles in the cytoplasmic leaflet of the nerve membrane apposed to a muscle fiber were present in vaguely linear aggregates (Fig. 24). These aggregates especially attracted our attention

FIGURE 26 Cytoplasmic leaflet of sarcolemma from a TTX-treated myotube. Arrows indicate several small clusters of the large angular particles associated with fluorescence. In addition, several large depressions (*D*) 110 nm in diameter are seen whose membrane contains particles similar in size, shape, and concentration to those found in the clusters. × 56,000.

FIGURE 27 Cross-fractured sarcoplasm of a control myotube. A probable membrane-bounded vesicle (arrow) located just below the sarcolemma (*S*) carries particles in the membrane leaflet which would merge with, or arise from, the cytoplasmic leaflet of the sarcolemma. The particles appear to be similar to those found associated with fluorescence, but the problems of shadowing the curved membrane make the diagnosis uncertain. × 130,000.

FIGURE 28 Cytoplasmic leaflet of sarcolemma from a control myotube. A depression (arrow) containing particles apparently of the type associated with fluorescence is immediately adjacent to an existing cluster (*C*). × 92,000.

since no such organization of paticles was seen either when no patch of particles was present in the muscle membrane or when the fracture plane passed through neuronal plasmalemma which was not apposed to the muscle (Fig. 25). Nerves can release transmitter from at least some regions of a nerve-muscle contact soon after such contact has been made (7, 8), so presumably active zone specializations exist at these regions. At any rate, it appears promising that specializations of the neuronal plasmalemma will serve as ultrastructural markers of functional neuromuscular junctions, thereby allowing us to study the sequence of events in synapse formation and development at a high level of resolution.

Mechanism of AChR Insertion

The mechanisms involved in AChR insertion into and removal from the sarcolemma, as well as the development and maintenance of high-density clusters of receptors, are still unknown. A current hypothesis is that of Palade (33, 34) who proposed that extracellular proteins are synthesized in the Golgi apparatus, transported to the cell surface in membrane-bounded vesicles, and subsequently released by exocytosis. Similarly, one might expect that membrane-bound proteins could likewise be synthesized in the Golgi apparatus and placed in the membranes of vesicles which would be transported to the cell surface. Merger of the vesicle membrane with the cell surface membrane would insert the membrane-bound proteins into that surface membrane. This mechanism was suggested for the AChR (17) and for electron-dense material in postsynaptic membranes (42). Rees et al. (43) have provided electron microscope evidence for such a mechanism, in sympathetic ganglion cells, involving vesicles ~100 nm in diameter. Vesicles of this size could account for the depressions containing particles which we have seen by freeze fracture (Figs. 12, 26, and 28).

In addition, Devreotes and Fambrough (12) have done electron microscope autoradiography on cultured rat muscle after purporting to label newly synthesized intracellular AChRs with ^{125}I-α-BGT. They claimed that a high proportion of specifically bound toxin was localized to the Golgi apparatus, accounting for AChR which, in earlier experiments, continued to appear on the cell surface after protein synthesis had been blocked. At this time we are uncertain whether the depressions actually represent insertion of new membrane into the sarcolemma or internalization of receptors to be degraded and/or transported. That we find more of these images in cultures grown in TTX, a treatment which increases the rate of receptor incorporation while leaving the rate of degradation unaffected (44), supports the first alternative, but experiments in which the TTX and TMR-α-BGT additions are carefully timed are needed to confirm this hypothesis.

APPENDIX

Quantitation of Cluster Sizes

Cluster Sizes in Control, TTX-Tested, and Innervated Myotubes

Particles were counted in a large sampling of clusters on control, TTX-treated, and innervated myotubes. The results are displayed as histograms in Fig. 29. In all conditions, progressively larger clusters (containing more particles) were progressively less common. However, the distribution of cluster sizes was skewed to the right (i.e., toward larger clusters) in places where clusters were grouped together, either in control myotubes or in innervated myotubes away from nerve contacts. There was little difference between these two distributions. However, the distribution was even more skewed toward larger clusters in TTX-treated myotubes and (in innervated myotubes) when clusters were adjacent to sites of nerve contact.

Distribution of Cluster Sizes

A histogram plot (Fig. 30) was made of the number of clusters containing successive numbers of particles from 2 to 91. Data were obtained from clusters occurring in groups of three or more in control and TTX-treated myotubes, as well as from myotubes in nerve-muscle co-cultures. For analysis, the histogram was first smoothed by finding the average number of clusters in nine consecutive sizes centered on 6, 10, 15, 20...80, 85 particles. The smoothed curve was fitted empirically to the exponential function $N_p = N_o \exp(-mp)$, where N_p is the number of clusters containing p particles and N_o and m are constants. Values for N_o and m were determined by least-squares regression of ln N_p on p. The resulting exponential, $N_p = 34.5 \exp(-0.0320p)$, is plotted as the solid line in Fig. 30. The smoothed curve was an excellent fit to the exponential (correlation coefficient $r = 0.99$).

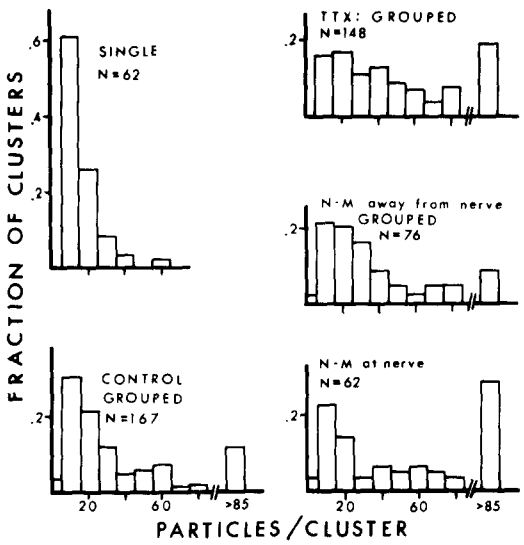

FIGURE 29 Histograms showing the distribution of cluster sizes (No. particles/cluster) found in the sarcolemma of myotubes cultured under various conditions. Clusters which were grouped together tended to be larger than those which occurred singly. The distribution was skewed toward larger clusters in sarcolemmas of myotubes which were TTX-treated or, in presumptively-innervated myotubes, for clusters grouped within 5 μm of a neurite-myotube contact. The statistical significance of the difference in distribution of clusters was determined by successive pairwise comparisons using the Kolmogorov-Smirnov test (13) on the raw data. The distribution of sizes of grouped clusters in myotubes of control cultures and in innervated myotubes >5 μm from neurite-myotube contact areas were not significantly different. All other distributions were significantly different from each other.

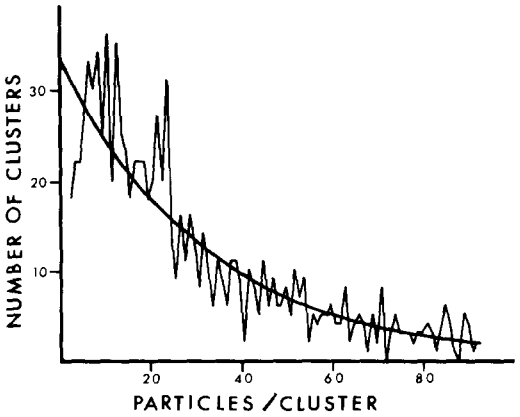

FIGURE 30 Histogram of the distribution of cluster sizes (No. particles/cluster) found in sarcolemmas of myotubes. Particles were counted in clusters occurring in groups of three or more in control (364 clusters; 3 myotubes), TTX-treated (396 clusters; 3 myotubes), and nerve-muscle cocultures (198 clusters; 4 myotubes). The number of clusters containing 2, 3, ... 91 particles was plotted. The heavy line is the best exponential fit to the combined data. See text for further details.

Data from each of the treatments also fitted exponential curves with slopes which varied somewhat from each other, as is suggested by the more condensed plot of portions of these data in Fig. 29. For this reason, the fact that the data fit exponential curves is more important than the actual parameters describing the curves. Data were combined in an effort to reduce random fluctuations and to establish, if they existed, true deviations from the exponential. Indeed the raw data were not a satisfactory fit to the exponential ($\chi^2 = 113$; $N = 90 - 3 = 87$; $p < 0.05$) due to the deficiency of small clusters (2–5 particles) and to the excess of clusters with 8, 10, 12, 14, 21, and 23 particles. Given the uncertainties in absolute identification of particles, however, it is unlikely that these individual peaks are significant. Nevertheless, the envelope of the histogram appears to depart from the smoothed curve in the ranges of 8–12 and 21–23 particles. Special effort was made to count the smallest clusters (2–5 particles), since they were less conspicuous than larger clusters. The cut-off point for histogram analysis was arbitrarily set at 91 particles. Large clusters (92–2,036 particles) also occurred, but only one or two examples of any particular size were found, which was insufficient for further quantitation.

Association of Particles

The association of large angular particles into clusters is a striking feature in membranes of myotubes. At least two explanations can be proposed for the association. First, the particles may have no affinity for each other; the clusters then represent chance associations of particles which are randomly scattered in the membrane. Second, the particles may have some affinity for each other of an (as yet) unspecified nature; clusters then result from this affinity.

Could Clusters of Particles Arise by Chance?

The likelihood of clusters of particles occurring by chance can be determined by a reverse of the procedure used to determine whether objects in a micrograph are randomly arranged (30). The total area is divided into equal-sized compartments, and

we ask whether the distribution of objects in the compartments is Poisson. We estimate 5% of the sarcolemmal area to contain clusters of large angular particles at a concentration of 3,500 particles/μm^2, while the remaining 95% of the area contains individual particles at a concentration of 10 particles/μm^2. The average concentration is then $0.05 \times 3.5 \times 10^3 + 0.95 \times 10 = 184$ particles/μm^2. If a 1-μm^2 area is divided into 200 boxes 5×10^{-3} μm^2 each, the average occupancy is 184/200, $\simeq 1$ particle/box. If particles were arranged randomly, occupancy of the boxes would follow the Poisson distribution, $n(k) = N \exp(-m)\, m^k/k!$, where $N = 184$ and $m = 1$. A box having the particle concentration of a cluster would have 5×10^{-3} $\mu m^2 \times 3.5 \times 10^3$ particles/$\mu m^2 = 18$ particles. The number of these arising if particles were arranged randomly would be $n(18) = 184 \exp(-1)\,(1)^{18}/18! = 2 \times 10^{-13}/\mu m^2$. In the approximately 10^4 μm^2 of sarcolemma we examined, this predicts $2 \times 10^{-13} \times 10^4$, or 2×10^{-9} clusters which is far fewer than actually observed. We conclude that the presence of clusters indicates that large angular particles are not randomly distributed in the sarcolemma.

Similar arguments can be used to determine the probability of the smallest clusters arising by chance association of individual particles in regions outside the existing clusters. Given the observed concentration of single particles, 10/μm^2, and again dividing 1 μm^2 of membrane into 200 boxes of area 5×10^{-3} μm^2, the average box contains $10/200 = 0.05$ particles, and the Poisson distribution predicts $N(2) = 10\ (0.05)^2 \exp(-0.05)/2! = 1.1 \times 10^{-2}/\mu m^2$. Since two particles sufficiently close together to be regarded as a cluster (concentration of 3,500 particles/μm^2) occupy only $2/3.5 \times 10^3$ $\mu m^2/5 \times 10^{-3}$ μm^2 or 0.11 of a box, the number of pairs of particles expected by chance is $0.11 \times 1.1 \times 10^{-2} = 1.3 \times 10^{-3}/\mu m^2$. In the approximately 10^4 μm^2 of sarcolemma examined, we would expect $10^4 \times 1.3 \times 10^{-3}$, or 13 pairs, somewhat less than were found (Fig. 27). Likewise the number of three-particle clusters expected by chance is $n(3) = 10\ (0.05)^3 \exp(-0.05)/3! = 2 \times 10^{-4}$. Of these, three particles at the density of a cluster occupy $3/3.5 \times 10^3/5 \times 10^{-3}$, or 0.17 of a box. The number of three-particle clusters expected by chance is then $0.17 \times 2 \times 10^{-4}/\mu m^2$, and in the 10^4 μm^2 of sarcolemma examined, we would expect 0.34 three-particle clusters. We actually found 23 such clusters, suggesting that these did not arise by chance association of individual particles. Similar arguments imply that all larger-size clusters cannot arise by chance association of individual particles.

Distribution of Cluster Sizes: Consideration of Equilibria

Since the chance association of particles cannot account for the number of clusters which are actually seen, such clusters must result from some net attraction of the particles for each other. Further analysis depends on the assumption that large clusters are "built up" by successive additions of single particles or small groups of particles. This is suggested by the fact that the membrane area in the largest clusters is too large to be added all-at-once to the sarcolemma and that the number of particles within a depression is much smaller than the number of particles in the largest clusters. Furthermore, cluster sizes can differ from each other by only one particle. Therefore, the accretion process can be written as a series of additions of k particles each to an original cluster of p particles:

$$p + k \rightleftarrows (p + k) + k \rightleftarrows (p + 2k) \ldots .$$

The additions are assumed to be reversible, and both p and k may be ≥ 1.

The distribution of cluster sizes seen in replicas represents a true equilibrium state if the rate of movement of particles into and out of the membrane is slower than the rate of translational movement of particles within the membrane. The available data suggest that this is true. Assuming the previous estimate of overall density of particles (184/μm^2) and a rate of addition of particles to the membrane which matches the rate of degradation (3% of receptors/h; reference 11), $184 \times 0.03 = 6$ particles/μm^2/h are added to and removed from the membrane. The rate of lateral diffusion can be obtained from the rough "diffusion constant" for membrane proteins in cultured rat myotubes of $D = 10^{-9}$ cm^2/s; reference 18). The mean square displacement, $\bar{x}^2 = 2\,Dt$, is 2×10^{-9} $cm^2/s \times 10^8$ $\mu m^2/cm^2 \times 60^2$ sec/h $= 7 \times 10^2$ μm^2/h. The average net translation is the square root of this or 26 μm/h, which is large compared to the size of the clusters. A comparably large value of 4 μm/h can be calculated from data on the movement of receptors labeled with fluorescent α-BGT (4).

For a constant amount of sarcolemma, the concentrations of clusters of sizes p, k, and p + k may be replaced by the numbers N_p, N_k, and N_{p+k} of such clusters which were observed. Assuming,

from the arguments given above, that equilibrium conditions prevail, the relationship between Gibbs free energy and the equilibrium constant can be written $\Delta G^\circ = -RT \ln (N_{p+k}/N_p \cdot N_k)$. The same equation (for $k = 1$) can be derived by considering clusters of any size p as being in equilibrium with p individual particles (cf. reference 51).

The actual distribution of cluster sizes fit an exponential curve, $N_p = N_o \exp(-mp)$, where N_p is the number of clusters of size p and N_o, m are constants. The ratio between the numbers of two clusters differing in size by k particles is, $N_{p+k}/N_p = \{N_o \exp[-m(p + k)]\}/N_o \exp[-mp] = \exp(-mk)$, which is a constant independent of p.

Substituting this result into the free energy-equilibrium relation, it is clear that the difference in free energy, ΔG°, is constant between any two clusters differing in size by k particles; in other words, the same amount of free energy change is involved in the addition of k particles to any size cluster. Both enthalpy and entropy changes contribute to the free energy change. The entropy contribution arises from the increased ordering of particles within a cluster, while the enthalpy contribution probably represents a balance between repulsion between the particles in a cluster and the stabilization of clusters of partially-hydrophilic receptor proteins within the hydrophobic lipid portion of the membrane. If the particles in a cluster are roughly hexagonally-closest-packed in a plane, a particle approaching the cluster would only interact with 3–5 particles of the cluster regardless of the cluster's size. Thus it is not unreasonable that the entropy and enthalpy changes, and therefore the free energy change, are similar or equal for the addition of particles to any size cluster.

The previous considerations indicate that raising the concentration of particles in the sarcolemma favors larger-size clusters by shifting the equilibrium to the right. A shift toward larger clusters is indeed found in TTX-treated myotubes (Fig. 29), where the total number of receptors is increased (44). The shift toward larger clusters in locations where they are grouped together (Fig. 29) could also result from a rise in the total number of receptors. The rise could be caused by receptors' being preferentially inserted into or stabilized at these areas.

We thank Dr. T. S. Reese for critical comments on the manuscript, Dr. Z. Vogel and Mrs. M. Towbin for TMR-α-BGT, Mrs. F. M. Neal for preparing the cultures, and Mrs. D. Connolly for typing the manuscript.

Received for publication 6 November 1978, and in revised form 7 March 1979

REFERENCES

1. AKERT, K., K. PFENNINGER, C. SANDRI, and H. MOOR. 1972. Freeze-etching and cytochemistry of vesicles and membrane complexes in synapses of the central nervous system. *In* Structure and Function of Synapses. G. D. Pappas and D. P. Purpura, editors. Raven Press, N. Y. 67–86.
2. ANDERSON, M. J., and M. W. COHEN. 1974. Fluorescent staining of acetylcholine receptors in vertebrate skeletal muscle. *J. Physiol.* **237:** 385–400.
3. ANDERSON, M. J., and M. W. COHEN. 1977. Nerve-induced and spontaneous redistribution of acetylcholine receptors on cultured muscle cells. *J. Physiol.* **268:**757–773.
4. AXELROD, D., P. RAVDIN, D. E. KOPPEL, J. SCHLESSINGER, W. W. WEBB, E. L. ELSON, and T. R. PODLESKI. 1976. Lateral motion of fluorescent-labeled acetylcholine receptors in membranes of developing muscle fibers. *Proc. Natl. Acad. Sci. U. S. A.* **73:**4594–4598.
5. BENNETT, M. V. L., G. D. PAPPAS, M. GIMENEZ, and Y. NAKAJIMA. 1967. Physiology and ultrastructure of electronic junctions. *J. Physiol.* **30:**236–300.
6. BETZ, W., and M. OSBORNE. 1977. Effects of innervation on acetylcholine sensitivity of developing muscle *in vitro*. *J. Physiol.* **270:**75–88.
7. COHEN, S. A. 1976. Early signs of transmitter release at neuromuscular junctions developing in culture. *Neuroscience.* **2:**1021*a*. (Abstr.).
8. COHEN, S. A., and G. D. FISCHBACH. 1977. Clusters of acetylcholine receptors located at identified nerve-muscle synapses *in vitro*. *Dev. Biol.* **59:**24–38.
9. COHEN, S. A., and D. W. PUMPLIN. 1977. Membrane structure of developing chick muscle fibers in regions with high affinity for α-bungarotoxin. *Soc. Neurosci. Symp.* **3:**214*a*. (Abstr.).
10. CROWE, L. M., and R. J. BASKIN. 1978. Freeze-fracture of intact sarcotubular membranes. *J. Ultrastruct. Res.* **62:**147–154.
11. DEVREOTES, P. N., and D. M. FAMBROUGH. 1975. Acetylcholine receptor turnover in membranes of developing muscle fibers. *J. Cell Biol.* **65:** 335–358.
12. DEVREOTES, P. N., and D. M. FAMBROUGH. 1978. Newly synthesized acetylcholine receptors are located in the Golgi apparatus. *J. Cell Biol.* **76:**237–244.
13. DIXON, W. J., and F. J. MASSEY. 1957. Introduction to Statistical Analysis. 2nd Ed. McGraw-Hill, N. Y.
14. DULHUNTY, A. F. and C. FRANZINI-ARMSTRONG. 1975. The relative contributions of the folds and caveolae to the surface membrane of frog skeletal muscle fibres at different sarcomere lengths. *J. Physiol.* **250:** 513–539.
15. ELLISMAN, M. H., J. E. RASH, L. A. STAEHELIN, and K. R. PORTER. 1976. Studies of excitable membranes. II. A comparison of specializations at neuromuscular junctions of mammalian fast and slow-twitch muscle fibers. *J. Cell Biol.* **68:**752–774.
16. EZERMAN, E. B., and H. ISHIKAWA. 1967. Differentiation of the sarcoplasmic reticulum and T system in developing chick skeletal muscle *in vitro*. *J. Cell Biol.* **35:**405–420.
17. FAMBROUGH, D. M. 1974. Cellular and developmental biology of acetlcholine receptors in skeletal muscle. *In* Neurochemistry of Cholinergic Receptors. E. deRobertis and J. Schacht, editors. Raven Press, N. Y. 85–113.
18. FAMBROUGH, D. M., H. C. HARTZELL, J. E. RASH, and A. K. RITCHIE. 1974. Receptor properties of developing muscle. *Ann. N. Y. Acad. Sci.* **228:**47–62.
19. FERTUCK, H. C., and M. M. SALPETER. 1976. Quantitation of junctional and extrajunctional acetylcholine receptors by electron microscope autoradiography after ^{125}I-α-bungarotoxin binding at mouse neuromuscular junctions. *J. Cell Biol.* **69:**144–158.
20. FISCHBACH, G. D. 1972. Synapse formation between dissociated nerve and muscle cells in low density cell cultures. *Dev. Biol.* **28:**407–429.
21. FISCHBACH, G. D., and S. A. COHEN. 1973. The distribution of acetylcholine sensitivity over uninnervated and innervated muscle fibers grown in cell culture. *Dev. Biol.* **31:**147–162.
22. FISCHBACH, G. D., S. A. COHEN, and M. P. HENKART. 1974. Some observations on trophic interaction between neurons and muscle fibers in cell culture. *Ann. N. Y. Acad. Sci.* **228:**35–46.
23. FRANK, E., and G. D. FISCHBACH. 1977. ACh receptors accumulate at newly formed nerve-muscle synapses *in vitro*. *In* Cell and Tissue Interactions. J. W. Lash and M. J. Burger, editors. Raven Press, N. Y. 285–291.
24. FRANZINI-ARMSTRONG, C., L. LANDMESSER, and G. PILAR. 1975. Size and shape of transverse tubule openings in frog twitch muscle fibers. *J.*

Cell Biol. **64**:493–497
25. HARTZELL, H. C., and D. M. FAMBROUGH. 1973. Acetylcholine receptor production and incorporation into membranes of developing muscle fibers. *Dev. Biol.* **30**:153–165.
26. HEUSER, J. E., T. S. REESE, and D. M. D. LANDIS. 1974. Functional change in frog neuromuscular junctions studied with freeze-fracture. *J. Neurocytol.* **3**:109–131.
27. HEUSER, J. E., and T. S. REESE. 1977. Structure of the synapse. *In* Handbook of Physiology—The Nervous System I. E. Kandel, editor. American Physiology Society, Washington, D. C. 261–294.
28. HEUSER, J. E., T. S. REESE, and D. M. D. LANDIS. 1974. Functional changes in frog neuromuscular junctions studies with freeze-fracture. *J. Neurocytol.* **3**:109–131.
29. KO, P. K., M. J. ANDERSON, and M. W. COHEN. 1977. Denervated skeletal muscle fibers develop discrete patches of high acetylcholine receptor density. *Science (Wash. D. C.).* **196**:540–542.
30. LAND, B. R., T. R. PODLESKI, E. E. SALPETER, and M. M. SALPETER. 1977. Acetylcholine receptor distribution on myotubes in culture correlated to acetylcholine sensitivity. *J. Physiol.* **269**:155–176.
31. MATTHEWS-BELLINGER, J. and M. M. SALPETER. 1978. Distribution of acetylcholine receptors at frog neuromuscular junctions with a discussion of some physiological implications. *J. Physiol.* **279**:197–213.
32. MCNUTT, N. S. and R. S. WEINSTEIN. 1973. Membrane ultrastructure at mammalian intercellular junctions. *Prog. Biophys. Mol. Biol.* **26**:45–101.
33. PALADE, G. E. 1959. Functional changes in the structure of cell components. *In* Subcellular Particles. T. Hayashi, editor. Ronald Press, N. Y., 64–83.
34. PALADE, G. E. 1975. Intracellular aspects of the process of protein synthesis. *Science (Wash. D. C.).* **189**:347–358.
35. PAULI, B. U., R. S. WEINSTEIN, L. W. SOBLE, and J. ALROY. 1977. Freeze fracture of monolayer cultures. *J. Cell Biol.* **72**:763–769.
36. PENG, H. B. and Y. NAKAJIMA. 1978. Membrane particle aggregates in innervated and noninnervated cultures of *Xenopus* embryonic muscle cells. *Proc. Natl. Acad. Sci. U. S. A.* **75**:500–504.
37. PEPER, K., F. DREYER, C. SANDRI, K. AKERT, AND H. MOOR. 1974. Structure and ultrastructure of the frog motor endplate. A freeze-etching study. *Cell Tissue Res.* **149**:437–455.
38. PRESCOTT, L., and M. W. BRIGHTMAN. 1976. The sarcolemma of *Aplysia* smooth muscle in freeze-fracture preparations. *Tissue Cell.* **8**:241–258.
39. PUMPLIN, D. W., and S. A. COHEN. 1978. Correlation of intramembranous particles with α-bungarotoxin binding in culture chick myotubes: quantization of particle clusters. *Soc. Neurosci. Symp.* **4**:772*a*. (Abstr.).
40. RASH, J. E., and M. H. ELLISMAN. 1974. Macrmolecular specializations of the neuromuscular junction and the nonjunctional sarcolemma. *J. Cell Biol.* **63**:567–586.
41. RASH, J. E., C. S. HUDSON, and M. H. ELLISMAN. 1978. Ultrastructure of acetylcholine receptors at the mammalian neuromuscular junction. *In* Cell Membrane Receptors for Drugs and Hormones. R. W. Straub and L. Bolis, editors. Raven Press, N. Y. 47–68.
42. REES, R. 1978. The morphology of interneuronal synaptogenesis. A review. *Fed. Proc.* **37**:2000–2009.
43. REES, R. P., M. B. BUNGE, and R. P. BUNGE. 1976. Morphological changes in the neuritic growth cone and target neuron during synaptic junction development in culture. *J. Cell Biol.* **68**:240–263.
44. SHAINBERG, A., S. A. COHEN, and P. G. NELSON. 1976. Induction of acetylcholine receptors in muscle cultures. Pfluegers Arch. *Eur. J. Physiol.* **361**:255–261.
45. SYTKOWSKI, A. J., Z. VOGEL, and M. W. NIRENBERG. 1973. Development of acetylcholine receptor clusters on cultured muscle cells. *Proc. Natl. Acad. Sci. U. S. A.* **70**:270–274.
46. TANFORD, C. 1974. Theory of micelle formation in aqueous solutions. *J. Phys. Chem.* **78**:2469–2479.
47. VOGEL, Z., and M. DANIELS. 1976. Ultrastructure of acetylcholine receptor clusters on cultured muscle fibers. *J. Cell Biol.* **69**:501–507.
48. VOGEL, Z., A. J. SYTKOWSKI, and M. W. NIRENBERG. 1972. Acetylcholine receptors of muscle grown *in vitro*. *Proc. Natl. Acad. Sci. U. S. A.* **69**:3180–3184.
49. YEE, A. G., G. Fischbach, and M. KARNOVSKY. 1976. Visualizing monolayers grown on glass coverslips prior to freeze-fracturing. *J. Cell Biol.* **70**(2, Pt. 2):155*a*. (Abstr.).
50. YEE, A. G., G. FISCHBACH, and M. KARNOVSKY. 1978. Clusters of intramembranous particles on cultured myotubes at sites that are highly sensitive to acetylcholine. *Proc. Natl. Acad. Sci. U. S. A.* **75**:3004–3008.